Biosensors and Bioelectronics 126 (2019) 590–595

Contents lists available at ScienceDirect

Biosensors and Bioelectronics

journal homepage: www.elsevier.com/locate/bios

Trace detection of some nitro-explosives using thermal mediated immunochemical defragmented method

Shilpa Chaudhary[a,c,1], Praveen Sonkusre[a,1], K.K. Bhasin[c], Priyanka Sabherwal[b,**], C. Raman Suri[a,*]

[a] CSIR-Institute of Microbial Technology, Sector 39-A, Chandigarh 160036, India
[b] Institute of Nano Science and Technology, Sector 64, Mohali 160062, India
[c] Department of Chemistry, Panjab University, Chandigarh 160014, India

ARTICLE INFO

Keywords:
Nitro-explosive
Hapten design
Specific antibodies
Thermolysis
Griess reagent
Colorimetric immunoassay

ABSTRACT

A new immunoassay format using thermally induced defragmentation of some nitro-explosives with a high degree of selectivity is reported. Specific antibodies against three widely used explosives, 2,4,6-trinitrotoluene (TNT), 1,3,5-trinitroperhydro-1,3,5-triazine (RDX), and pentaerythritol tetranitrate (PETN) were generated by designing suitable haptens using geometry optimization modules. These in-house generated antibodies were used in a newly developed thermal mediated immunochemical biosensing technique which involves the binding of specific antibodies to respective nitro-explosives on a microtiter strip, resulting in the formation of specific immunocomplex. Heating the specific immuno-complex formed on microtiter wells resulted in thermal lysis of nitro-explosives to generate nitrite ions. These ions react with Griess reagent to form a colored chromophore which correlates the concentration of individual explosive in the sample. The present work fulfills the need for an improved explosive detecting system that is highly specific and capable of quickly determining the presence of nitrate containing explosives from a mixture pool.

1. Introduction

Nitrate containing explosives, such as TNT, RDX and PETN are important environmental, security and health concern for the global community because of their extensive usages, storage, testing, and disposal (Che et al., 2012; Sulzer et al., 2012). Current methods for the detection of these explosives are usually performed off-site, involving complex instrumentation, and are not suitable for field applications (Rose et al., 2005; Jiang et al., 2008; Germain and Knapp, 2009). Consequently, detection strategies are trending towards the development of portable techniques such as chemosensors and biosensors, which are reliable and sensitive enough to evaluate the presence of explosives in field conditions (Shangguan et al., 2008; Wang et al., 2012).

In recent years, affinity-based assays using specific biorecognition elements such as antibodies or aptamers are gaining importance, and becoming a preferential alternate approach for explosives detection in virtue of their high selectivity, sensitivity, and rapidness (Pang et al., 2014; Priyanka et al., 2014; Zhang et al., 2015). In one of the earlier studies, Gauger and colleagues reported analysis of explosives in contaminated soil samples using a displacement based immunoassay (Gauger et al., 2001). Few year later, Mulchandani and his team reported a sensitive single-walled carbon nanotubes based chemiresistive immunosensor for label-free detection of TNT (Park et al., 2010). Recently, our group has also reported screening of highly specific aptamers against TNT, and used these biorecognition elements along with in-house generated anti-TNT antibodies in an apta-immuno FRET-based assay format for TNT detection (Sabherwal et al., 2014). This reported sensing platform showed good sensitivity with a detection limit of 0.4 nM, but having some drawback of using costly reagents and complex instrumentation. To make the sensing platform more simpler, rapid and cost-effective without loosing its specificity, we herein demonstrate a new immunochemical sensing strategy which is based on thermally induced lysis of nitro-explosives. It has been reported by Andrew and Swager that during the thermo lysis of some nitro-explosives in liquid samples, different reactive species like NO_3^-, NO_2^-, NO_2^+, and $NO_2^{\cdot}$ are generated which react quickly with the sensor molecules leading to the formation of a highly fluorescent product or a colored azo complex

* Correspondence to: CRF, IIT Ropar, Rupnagar, Punjab 140001, India.
** Correspondence to: Bigtec Labs,2nd Floor, Golden Heights, 59th 'C' Cross,, 59, 4th M Block, Rajaji Nagar, Bengaluru, Karnataka 560010, India.
E-mail addresses: priyanka.s@bigtec.co.in (P. Sabherwal), crsuri@iitrpr.ac.in (C.R. Suri).
[1] Both authors contributed equally.

https://doi.org/10.1016/j.bios.2018.09.043
Received 25 July 2018; Received in revised form 2 September 2018; Accepted 12 September 2018
Available online 18 September 2018
0956-5663/

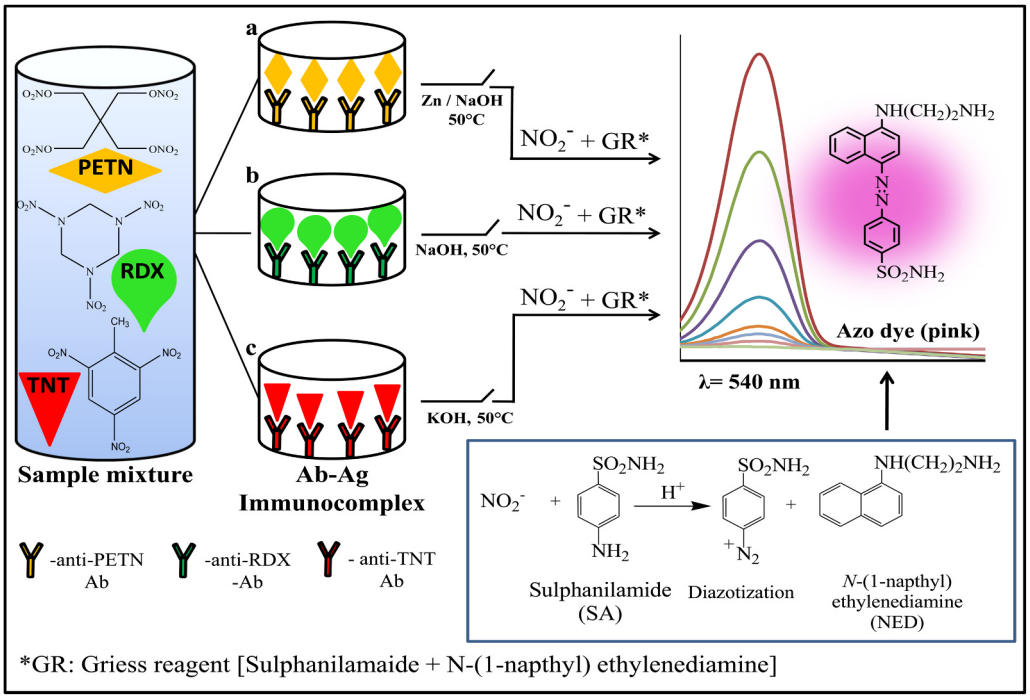

Scheme 1. Schematic showing the sequential detection of explosives in a mixture pool utilizing specific antibodies against targeted explosives (a: PETN, b: RDX, and c: TNT).

using Griess reagent (Andrew and Swager, 2011). However, the associated problem was its selectivity since decomposed reactive products from all explosives or similar compounds react with the sensor molecule. To improve the detection efficiency and selectivity, we have developed a new heterogeneous immunochemical based detection strategy that make use of specific antibodies against all three explosives (PETN, RDX and TNT) coated on microtiter wells. Thermolysis of individual nitro-explosive bound to respective antibodies generate nitrite ions which resulted a colored chromophore by adding nitrite specific Griess reagent (Scheme 1). To the best of our knowledge, this is the first report of a direct immunoassay format where thermo-lysis of nitro-explosives or any other nitro-substances from the formed immuno-complex have been used for their detection (Patent filed).

2. Materials and methods

2.1. Materials

Analytical standards of TNT, PETN, RDX, 2,4-dinitrotoluene (DNT), 4-nitrotoluene (MNT), 2,4-dinitrophenol (DNP), 4-nitrophenol (NP), *tert*-butylamine, nitromethane, fuming nitric acid, deuterated dimethylsulphoxide ($(CD_3)_2SO$), glutaric anhydride, 4-dimethylaminopyridine (4-DMAP), bovine serum albumin (BSA), *N,N′*-dicyclohexylcarbodiimide (DCC), *N*-hydroxysuccinimide (NHS), Griess reagent (Sulfanilamide (SA), *N*-(1-napthyl)ethylene diamine dihydrochloride (NED), protein A and 2-methyl-3,5-dinitro-benzoic acid were purchased from Sigma Chemical India. F8 Maxisorp Nunc-Immuno Module strips were purchased from Thermo Scientific. Milli-Q ultrapure water having a resistivity of ≥ 18 MΩ.cm was used for the preparation of all buffers and solutions.

2.2. Haptens synthesis and bio-conjugation

An analog of PETN (hapten), pentaerythritoltrinitrate (PET3N), was synthesized by nitration of pentaerythritol (Andrew and Swager, 2007) followed by the reaction with glutaric anhydride. For this, 0.5 g PET3N was mixed with glutaric anhydride in 15 mL acetonitrile (ACN) at equimolar concentration. 4-(dimethylamino)pyridine (4-DMAP) was added to it in 0.5 M excess and refluxed for 24 h. After completion of the reaction, the solvent was evaporated and product was purified with a silica column using ethyl acetate-hexane as a solvent system. The purified product was characterized using FT-IR, NMR, and Mass spectroscopy techniques. Hapten for RDX was synthesized as described by Blackburn et al. (2000). The final product extracted in ethyl acetate was purified through a silica column using the chloroform-methanol solvent system and characterized with FT-IR and Mass spectroscopy. 2-methyl-3,5-dinitro-benzoic acid (Sigma, USA) was used as a hapten for TNT. Synthesized haptens for all three explosives (PETN, RDX and TNT) were further conjugated with a carrier protein (BSA) at optimum molar ratios using DCC/NHS coupling chemistry as described earlier (Singh et al., 2004). The hapten-protein conjugation density (no. of hapten per protein molecule) was confirmed by characterizing the conjugate with fluorescence, electrophoresis and mass spectrometric techniques (Supporting information ST1; 1a-3a). The fluorescence spectra of hapten-protein conjugates were recorded from 300 nm to 450 nm with maxima at 340 nm by exciting the tryptophan residues present in the protein at 290 nm using Varian Cary Eclipse fluorescence spectrophotometer. For mass analysis, 1 mg/mL conjugate was first mixed with equal proportion of sinapinic acid solution (10 mg/mL in 50% ACN containing 0.1% trifluoroacetic acid), and coated on MALDI sample plate. After drying, mass spectra of hapten-protein conjugates were recorded on AB SCIEX 5800 MALDI TOF/TOF spectrophotometer.

2.3. Anti-PETN, anti-RDX, and anti-TNT antibodies production

The antibodies were raised in rabbits according to the earlier reported protocol (Singh et al., 2004) in compliance with the Institutional Animal Ethics Committee guidelines. 300 μg of hapten-protein conjugates of PETN, RDX, and TNT (at optimal hapten-protein molar ratio 1:50) were injected subcutaneously in three different New Zealand white (NZW) rabbits to generate anti-PETN, anti-RDX, and anti-TNT antibodies, respectively. The collected sera were processed, and IgG antibodies were purified by affinity chromatography using protein A column, and used for assay development.

Table 1
The predicted correlation coefficient of QSAR descriptors for PETN, RDX and TNT calculated from their minimum energy configurations by using Chem3D Pro 11.0 and Hyperchem software. Energy minimized structures of all three explosives using ChemBio software and (E_{HOMO} and E_{LUMO}) obtained from the frontal orbital energy diagrams.

S.No	QSAR Properties	PETN	RDX	TNT
1	Structure	 Mol. wt. 316.01	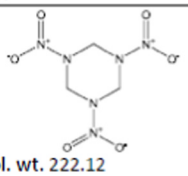 Mol. wt. 222.12	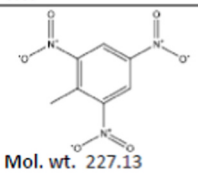 Mol. wt. 227.13
2	Total Energy (kcal/mol)	-106628.4496913	-73167.9084157	-72552.2609054
3	Heat of Formation (kcal/mol)	91.2545887	40.3252883	3.0451036
4	Dipole (Debyes)	7.46	5.5	1.380
5	Log P	-4.65	3.46	-7.37
6	Hydration Energy (kcal/mol)	-24.17	-12.34	
7	Refractivity (A^{03})	41.28	37.87	45.13
8	Polarizability (A^{03})	15.16	15.08	14.66
9	Orbitals (LUMO)	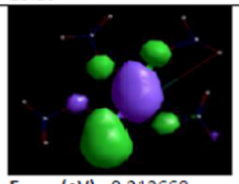 E_{LUMO} (eV) -8.213668	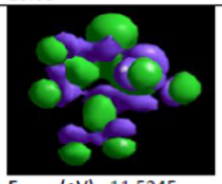 E_{LUMO} (eV) -11.5245	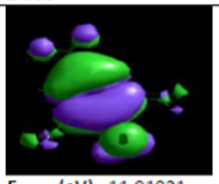 E_{LUMO} (eV) -11.91831
10	Orbitals (HOMO)	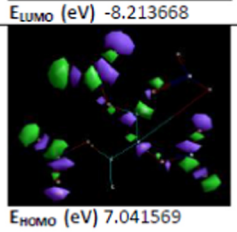 E_{HOMO} (eV) 7.041569	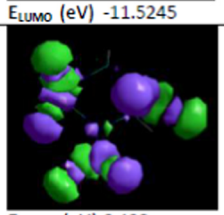 E_{HOMO} (eV) 6.438	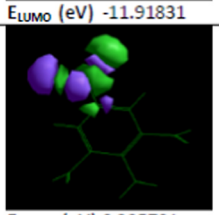 E_{HOMO} (eV) 6.225721

2.4. Defragmentation of nitro explosives: assay optimization

During the thermo lysis of selected nitro-explosives (PETN, RDX, and TNT), different reactive species like NO_3^-, NO_2^-, NO_2^+, and $NO_2^{\cdot}$ are generated (Andrew and Swager, 2011). Various reaction conditions such as temperature, time, pH, and catalyst were optimized for the maximum generation of NO_2^- from the respective explosives. In the case of thermo lysis of PETN, reactive species like $NO_2^{\cdot}$ and NO_2^+ are also reported to generate along with NO_2^-. For this, zinc dust was used as a reducing agent converting NO_3^- to NO_2^-. The concentration of zinc dust was optimized using different conc. of PETN (5, 0.5, and 0.05 ppm in 50% ACN respectively). To determine the suitable solvent for nitro-explosive defragmentation, three different solvents viz., ACN, dimethylsulphoxide, and water were tested. 50% ACN showed highest defragmentation efficiency for all three nitro-explosives, and hence used for further experiments. Details of all above optimization conditions are given in Supporting information (ST2 a-c; Figs. S4-S8). Further, the extent of nitrite ions after defragmentation from respective explosives (PETN, RDX and TNT) was confirmed by electrochemical analysis of nitrite peaks of all the samples recorded at 0.8 V (*Vs* Ag/AgCl reference electrode) (Badea et al., 2001) in the form of differential pulse voltammogram on a CHI660D EC workstation with a scan rate of 0.004 V from 0 to 1.4 V on screen-printed electrodes (Supporting information ST2 d).

2.5. Immunochemical defragmentation assay development

Microtiter strips (8-wells) were first coated with 300 µL of Protein A at a concentration of 5 µg/mL prepared in 100 mM carbonate buffer (pH 9.4) for overnight at 4 °C, and then washed thrice with 50 mM phosphate buffer (pH 7.2). 300 µL of anti-explosives antibodies (anti-PETN, anti-RDX, and anti-TNT respectively) prepared in carbonate buffer (100 mM, pH 9.4) at a concentration of 5 µg/mL was added to the respective wells (in triplicate) of strip and incubated for 2 h at RT. After washing the strips with PB, standard solutions of PETN, RDX, and TNT prepared in 50% ACN were added to the respective antibodies coated wells at different concentrations, and strips were kept for incubation at RT for 1 h followed by washing with buffer. On PETN treated wells, 100 µg zinc dust was added, followed by addition of 83 mM of 1 M NaOH. However, RDX and TNT coated wells were added respectively with 90 mM of 1 M NaOH and 75 mM of 1 M KOH. The volume of each well was adjusted to 300 µL using 50% ACN. Strips were incubated at 50 °C for 20 min for thermal lysis of nitro groups from the bound antibody-explosive immune-complex, followed by adding 100 µL of Griess reagent into each well for color formation. The strips were read at 540 nm.

3. Results and discussion

3.1. Hapten design, bioconjugation and antibodies generation

Highly specific bioreceptors (anti-PETN, anti-RDX, and anti-TNT antibodies) were generated in-house in NZW rabbits by designing suitable haptens (Supporting information; Figs. ST 1–3). The respective hapten molecules (analogs of PETN, RDX, and TNT) were designed based on minimum energy confirmations studies using geometry optimization modules in ChemBio 3D 11.0 and Hyperchem 8. Molecular mechanics force field MM2 was used (ChemBio3D, minimum rms ~ 0.042 kJ mol $Å^{-1}$) to pre-optimize the hapten structures. Austin model 1 (AM1) semi-empirical quantum chemical method was used to obtain minimum energy conformations until the root mean square (RMS) of the gradient became less than 0.021 kJ/mol 3 Å (Hyperchem, 585

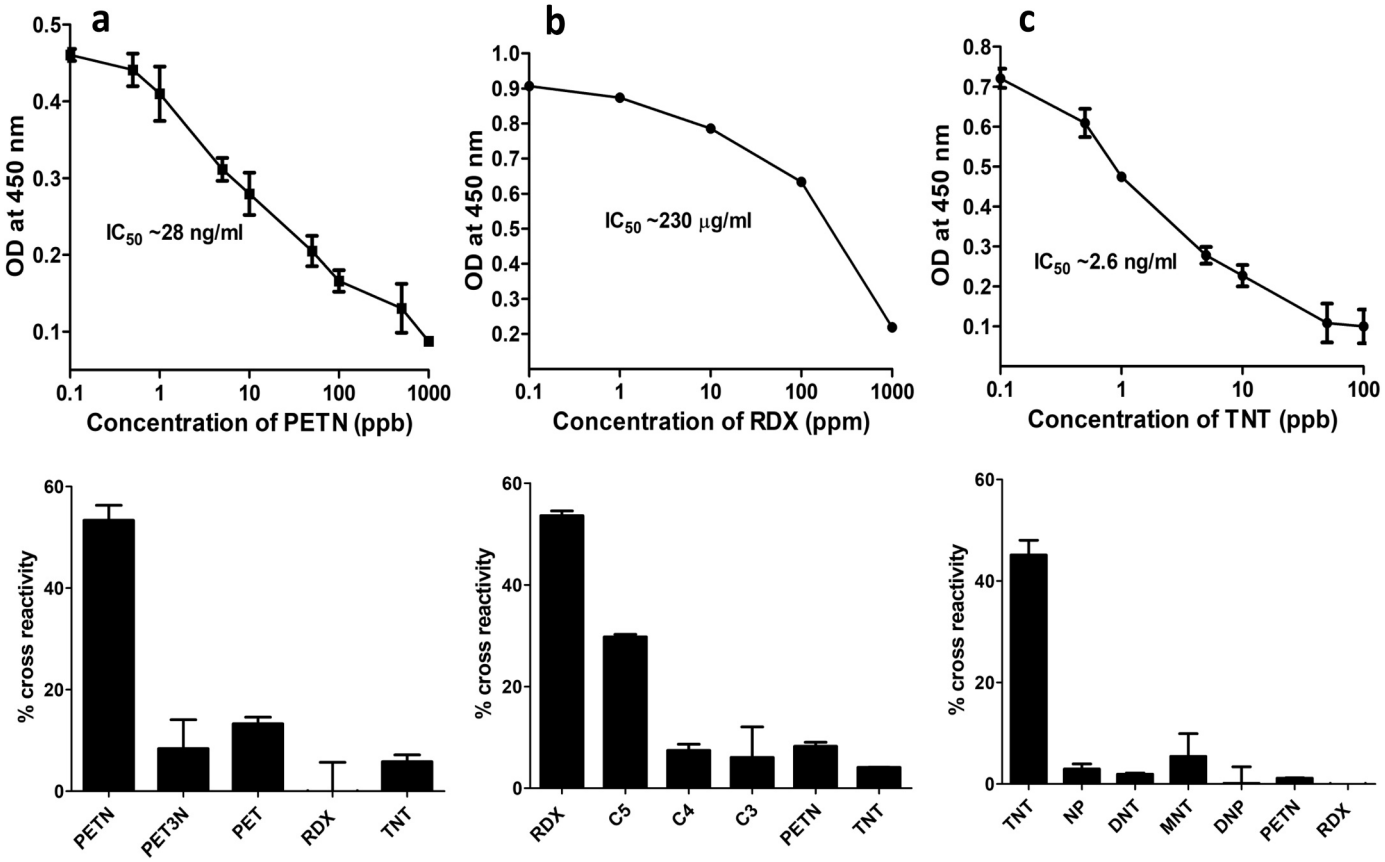

Fig. 1. Inhibition curves for determining the sensitivity of (a) anti-PETN, (b) anti-RDX, and (c) anti-TNT antibodies. The IC_{50} values in the inset were determined by taking 50% inhibition. Respective bottom bar diagrams show the percentage cross-reactivity of anti-PETN, anti-RDX, and anti-TNT antibodies with respect to other explosives and their respective analogs.

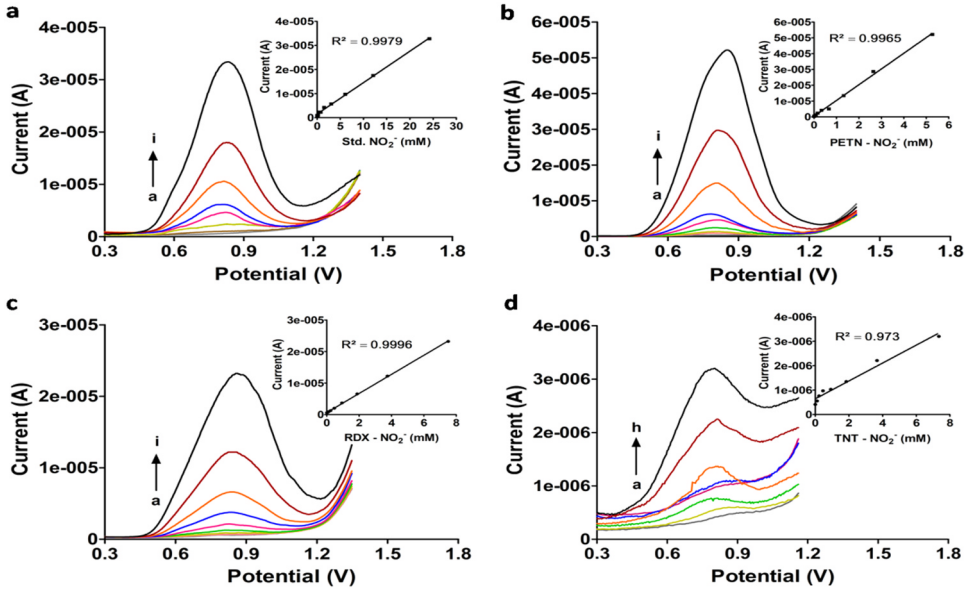

Fig. 2. Differential pulse voltammograms represent oxidation peak of nitrite ions. (a) standard $NaNO_2$ solution, (b) PETN, (c) RDX, and (d) TNT represent the nitrite ions generated after their respective thermolysis. Inset graph showing the calibration curves of individual analytes.

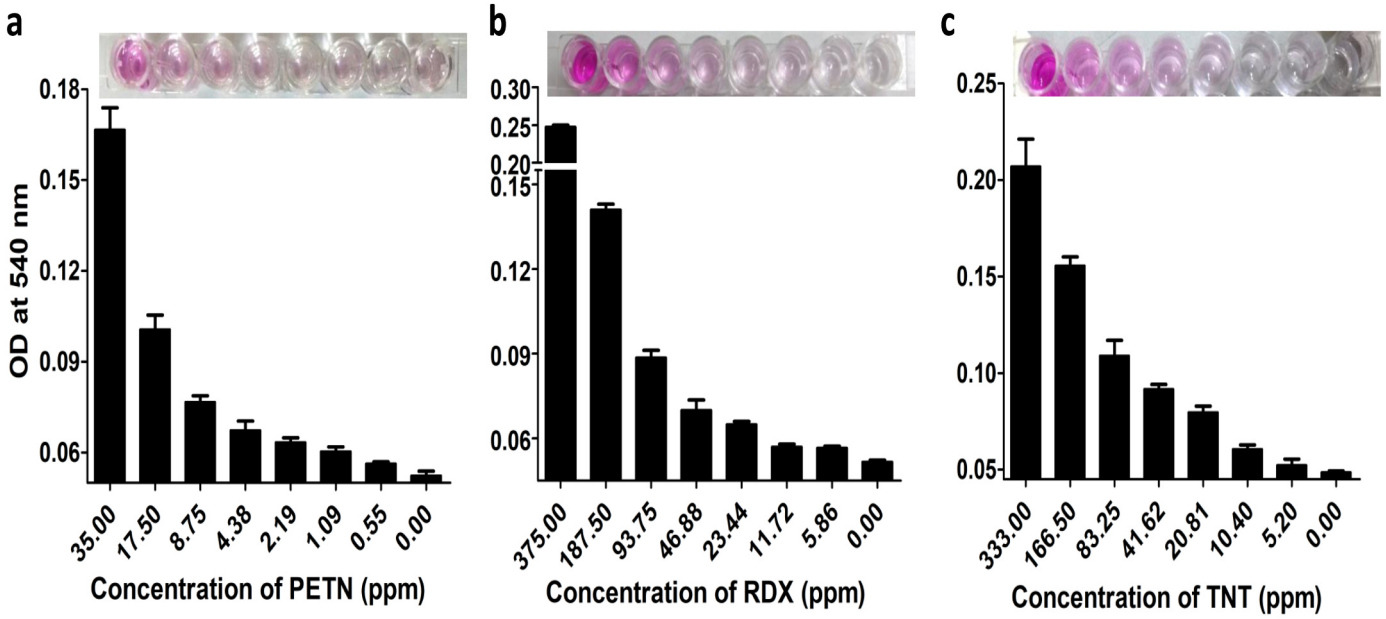

Fig. 3. Colorimetric determination of explosives (a) PETN (a), (b) RDX (b), and (c) TNT (c) after thermal treatment (20(20 min) of the antibodies-explosive complex. Inset shows the formation of a chromophore of different colored intensity. The error bars represent the standard deviation of the mean. (For interpretation of the references to color in this figure legend, the reader is referred to the web version of this article.)

maximum cycles). Quantitative structure-activity relationship (QSAR) studies were carried out on the basis of the energy-minimized structures using QSAR descriptors such as total energy, heat of formation, polarizability, hydration energy, log of the octanol/water partition coefficient (log P), refractivity, the lowest unoccupied molecular orbital energy (E_{LUMO}), the highest occupied molecular orbital energy (E_{HOMO}) (Table 1). The calculated parameters were used to confirm the mimicness of the designed hapten with the targeted explosive molecules. These studies were carried out to obtain insights about antibody recognition towards the target analyte .The above parameters with respect to the Hansch equation (Hansch, 1969), suggesting the increased predictive ability of the structural activity by introducing hydrophobic, electrical, and steric parameters as below:

$$\log 1/C = k_1 \log P + k_2(\log P)^2 + k_3\sigma + k_4 Es + k$$

where log 1/C is the logarithm of the biological activity value; log P is the logarithm of the octanol/water partition coefficient; Es is the Taft steric parameter; σ is the Hammett electrical parameter. From the Hansch equation, $(\log P)^2$ and log P were used to represent the hydrophobicity of targeted explosives and the respective haptens. The result of correlation analysis showed that the Pearson's coefficient correlation r = 0.9 with the experimental IC_{50}. It was also observed that in all the three selected explosives, the frontal (E_{HOMO}) is more localized over $–NO_2$ groups and thereby favor more antigen-antibody interactions (Sabherwal et al., 2014).

Based on these theoretical studies, the respective hapten molecules were synthesized, purified, and characterized. FT-IR analysis of PETN hapten prepared in KBr pellet showed peaks at ν_{max} (cm^{-1}) 1734, 1707 (C=O str), 1635 (NO_2 str) 2954 (C-H str) in Brucker Vertex-70 FT-IR spectrometer using opus software. NMR spectrum was recorded in $(CD_3)_2SO$ solvent using JEOL NMR instrument of 300 MHz and the peaks were obtained at δ_H [$(CD_3)_2SO$] 1.7 (2 H, m), 2.21 (2 H, t), 2.32 (2 H, t), 4.14 (2 H, s), 4.65 (6 H, s). A mass spectrum analysis on the Agilent 6550 QTOF LC/MS system performed on ESI ionization mode with the fragmentor voltage of 150 V showed a peak at *m/z* 389 (M^{+3}). FT-IR and Mass spectroscopy analysis of RDX hapten showed ν_{max} (cm^{-1}) 1752, 1719 (C=O str), 1277 (C-O str), 1573 (NNO_2 str), 1390 (NO_2 str), 2924, 3037 (C-H str), 3444 (OH str) and *m/z* (LCMS-ESI) 363(M^{-2}), 364 (M^{-1}), 365 (M) respectively.

These in-house synthesized haptens were conjugated with a carrier protein (BSA) at optimum molar ratios using DCC/NHS coupling chemistry (Singh et al., 2004), and characterized by fluorescence, electrophoresis, and mass spectrometric techniques to determine the hapten-protein conjugation density (Supporting Fig. S1-S3). Antibodies generated with these characterized hapten-protein conjugates showed excellent sensitivity with a half maximal inhibitory concentration (IC_{50}) of 28 ng, 230 μg, and 2.6 ng for PETN, RDX, and TNT respectively (Fig. 1). These antibodies were subsequently used in our newly developed immunoassay format.

3.2. Optimization of defragmentation efficiency of nitro-explosives in liquid samples

The thermolysis of nitro-aromatic, nitroester and nitramine-based energetic compounds under various conditions has been studied and found to produce a number of nitro based degradation products, including nitrate, nitrite or nitrous oxide (Pesenti et al., 2014). The suggested thermolysis degradation mechanisms for PETN imply the cleavage of the $O\text{-}NO_2$ bond in PETN which initially produces an alkoxide and highly reactive nitrate ions. In this case, the highly reactive nitrate ions are converted to nitrite using optimum concentrations of a metallic catalyst (zinc dust). 100 μg Zn dust has shown best catalytic activity for the reduction of $–NO_3^-$ to NO_2^- in the standard PETN test samples prepared in 50% ACN at pH 10 (maintained with 1 N NaOH). In the case of RDX, evidence of both the homolytic and heterolytic scission of the $N\text{-}NO_2$ bond to produce nitrogen dioxide or nitrite respectively are reported (Zeller, 1955). Further, enhancement of heterolytic scission of $N\text{-}NO_2$ of RDX samples was carried out at a higher temperature (thermal defragmentation) for different time intervals using standard RDX samples (Supporting information; Figs. S5 and S6). However, the reaction of TNT compound with hydroxide ions rely on the Janowski reaction resulted in the formation of Meisenheimer complex, which is responsible for the intense adsorption of visible light giving the hydrolysate a deep yellow color. Further, alkaline hydrolysis of TNT followed by thermal treatment results in the splitting of nitrite ion in presence of hydroxide ions (Saupe et al., 1998) (Supporting information; Fig. S7). The amount of transformed nitrite in above conditions from all three explosives (PETN, RDX, and TNT) was measured by

reacting with Griess reagent forming a pink color in the presence of acids (Supporting infomation ST3), which was detected photometrically at 540 nm.

To reconfirm the thermal defragmentation and generation of NO_2^- from the nitro-explosive samples, NO_2^- were determined electrochemically on a CHI660D electrochemical workstation using $NaNO_2$ as a standard solution for NO_2^-. Differential pulse voltammogram of all the samples showed distinct nitrite oxidation peaks at 0.8 V (Ag/AgCl reference electrode) confirming the presence of NO_2^- (Fig. 2). The presence of nitronium ions, also produced in the reaction was investigated using linear sweep voltammetry (LSV). Insignificant amount of nitronium in comparison to the nitrite ions was observed (Supporting information; ST4 and Fig. S8).

3.3. Thermal mediated immunochemical defragmented assay

Experimentally obtained optimum conditions for the maximum NO_2^- generation from the individual explosive was used in the antibody-based direct immunoassay format. Thermal lysis of bound nitro-explosives from respective immune-complexes at 50 °C produced highly reactive nitrogen oxide species (NO_x) (Andrew and Swager, 2011). This could transform sulfanilamide present in the Griess reagent to diazonium cation, to form a pink colored chromophore on reaction with NED (Supporting information ST4). A gradual increase in the color of the formed product with the increase in concentrations of respective explosives PETN, RDX, and TNT, respectively) was observed (Inset of Fig. 3). Optical density (OD) measured at 540 nm further confirms the linear increase in color intensity with concentrations of respective explosives. A detection limit of 1.19, 2.7, and 2.97 ppm, respectively was achieved with PETN, RDX, and TNT, respectively. The applicability of developed assay format was further validated by using soil samples (5 g) spiked with 5 mg of each PETN, RDX, and TNT samples respectively as per protocol developed by Anilanmert et al. (2016) (Supporting information; ST5; Fig. S9).

4. Conclusions

The newly developed thermal mediated immunochemical defragmented method allows direct detection of nitro-explosives individually in sequential manner with high degree of specificity. Practically useful detection limit for all three explosives viz. PETN, RDX, and TNT was of the order of 1.19, 2.7, and 2.97 ppm respectively with almost insignificant cross-reactivity problem with other explosives or analogs. The present work thus fulfills the need for an improved explosive detecting system that is specific, accurate and capable of quickly determining the presence of nitrate containing explosives in desired range.

Acknowledgments

Authors thank the office of Principal Scientifc Advisor to Government of India through Department of Science and Technology, India, and the Council of Scientific and Industrial Research (CSIR), India for financial support. SC also acknowledges CSIR for SRF fellowship (121359/2K15/1).

Appendix A. Supporting information

Supplementary data associated with this article can be found in the online version at doi:10.1016/j.bios.2018.09.043.

References

Andrew, T.L., Swager, T.M., 2007. J. Am. Chem. Soc. 129 (23), 7254–7255.
Anilanmert, B., Aydin, M., Apak, R., Avci, G.Y., Cengiz, S., 2016. Anal. Sci. 32, 611–616.
Andrew, T.L., Swager, T.M., 2011. J. Org. Chem. 76 (9), 2976–2993.
Badea, M., Amine, A., Palleschi, G., Moscone, D., Volpe, G., Curulli, A., 2001. J. Electroanal. Chem. 509 (1), 66–72.
Blackburn, G.M., Beadham, I.G., Adams, H., Hutchinson, A.P., Nicklin, S., 2000. J. Chem. Soc. Perkin Trans. 1 (2), 225–230.
Che, Y., Gross, D.E., Huang, H., Yang, D., Yang, X., Discekici, E., Xue, Z., Zhao, H., Moore, J.S., Zang, L., 2012. J. Am. Chem. Soc. 134 (10), 4978–4982.
Gauger, P.R., Hault, D.B., Patterson, C.H., Charles, P.T., Shriver-Lake, L., Kusterbeck, A.W., 2001. J. Hazard. Mater. 3 (1–2), 51–63.
Germain, M.E., Knapp, M.J., 2009. Chem. Soc. Rev. 38 (9), 2543–2555.
Hansch, C., 1969. Acc. Chem. Res. 2, 232–239.
Jiang, Y., Zhao, H., Zhu, N., Lin, Y., Yu, P., Mao, L., 2008. Angew. Chem. 47 (45), 8601–8604.
Pang, S., Labuza, T.P., He, L., 2014. Analyst 139 (8), 1895–1901.
Park, M., Cella, L., Chen, W., Myung, N.V., Mulchandani, A., 2010. Biosens. Bioelectron. 26 (4), 1297–1301.
Pesenti, A., Taudte, R.V., McCord, B., Doble, P., Roux, C., Blanes, L., 2014. Anal. Chem. 86 (10), 4707–4714.
Priyanka, Shorie, M., Bhalla, V., Pathania, P., Suri, C.R., 2014. Chem. Commun. 50 (9), 1080–1082.
Rose, A., Zhu, Z., Madigan, C.F., Swager, T.M., Bulovic, V., 2005. Nature 434 (7035), 876–879.
Sabherwal, P., Shorie, M., Pathania, P., Chaudhary, S., Bhasin, K.K., Bhalla, V., Suri, C.R., 2014. Anal. Chem. 86 (15), 7200–7204.
Saupe, A., Garvens, H.J., Heinze, L., 1998. Chemosphere 36 (8), 1725–1744.
Shangguan, D., Meng, L., Cao, Z.C., Xiao, Z., Fang, X., Li, Y., Cardona, D., Witek, R.P., Liu, C., Tan, W., 2008. Anal. Chem. 80 (3), 721–728.
Singh, K.V., Kaur, J., Varshney, G.C., Raje, M., Suri, C.R., 2004. Bioconj. Chem. 15, 168–173.
Sulzer, P., Petersson, F., Agarwal, B., Becker, K.H., Jurschik, S., Mark, T.D., Perry, D., Watts, P., Mayhew, C.A., 2012. Anal. Chem. 84 (9), 4161–4166.
Wang, Y., La, A., Bruckner, C., Lei, Y., 2012. Chem. Commun. 48 (79), 9903–9905.
Zeller, H.D., 1955. Analyst 80 (9), 632–633.
Zhang, Q., Zhang, D., Lu, Y., Yao, Y., Li, S., Liu, Q., 2015. Biosens. Bioelectron. 68, 494–499.